

Compressible Problem

A grid of 35×35 cells is used with Neumann boundary conditions only. The domain consists of layers with two different permeability values (see Figure 1). The first layer has a permeability of $\sigma_1 = 30mD$, and the permeability of the second layer is $\sigma_2 = 3mD$. Therefore the permeability contrast between the layers is 10^{-1} . The initial pressure of the reservoir is set as 200 bars. Four wells are positioned in the corners of the domain with a bhp of 100 bars, and a well is placed in the center of the domain with a bhp of 600 bars. For the first set of problems, we use the updated solution of the first 10 time steps with the same configuration as the problem as deflation vectors. We solve the rest of the time steps with DICCG₁₀ method with the 10 snapshots as deflation vectors, DICCG_{POD}. For the second set of experiments, we use the same configuration as in the original problem but we vary the configuration of the wells. One corner well has the same pressure as the reservoir (200 bar), the other corner wells have a pressure of 100 bars and the central well has a pressure of 500 bars.

System configuration

Initial pressure 200 bar.

$W1 = W2 = W3 = W4 = 100$ bar.

$W5 = 600$ bars.

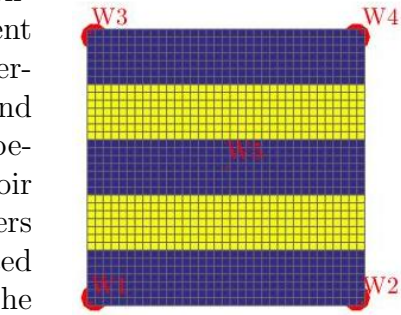


Figure 1: Heterogeneous permeability, 5 wells, compressible problem.

and with 5 basis POD vectors as deflation vectors, DICCG_{POD}. For the second set of experiments, we use the same configuration as in the original problem but we vary the configuration of the wells. One corner well has the same pressure as the reservoir (200 bar), the other corner wells have a pressure of 100 bars and the central well has a pressure of 500 bars.

Boundary conditions :

$$\frac{\partial P(y=1)}{\partial n} = \frac{\partial P(y=ny)}{\partial n} =$$

$$\frac{\partial P(x=1)}{\partial n} = \frac{\partial P(x=nx)}{\partial n} = 0.$$

Snapshots (second set of experiments)

z_1 : $W2 = W3 = W4 = 100$ bars, $W1 = 200$ bars, $W5 = 500$ bars.

z_2 : $W1 = W3 = W4 = 100$ bars, $W2 = 200$ bars, $W5 = 500$ bars.

z_3 : $W1 = W2 = W4 = 100$ bars, $W3 = 200$ bars, $W5 = 500$ bars.

z_4 : $W1 = W2 = W3 = 100$ bars, $W4 = 200$ bars, $W5 = 500$ bars.

The simulation was performed during 152 days with 52 time steps and a time step of 3 days. The tolerance of the NR method and the linear solvers is 10^{-5} .

Case 1

In Figure 78, the solution obtained with the ICCG method is presented, the solution is the same for all methods. The upper left figure represents the pressure field at the final time step. The upper right figure represents the pressure across the diagonal joining the (0,0) and (35,35) grid cells for all the timesteps. We observe the initial pressure (200 bars) in this diagonal and the evolution of the pressure field through time. In the lower figure we observe the surface volume rate for the five wells during the simulation.

1 Accuracy NR iteration 10^{-4}

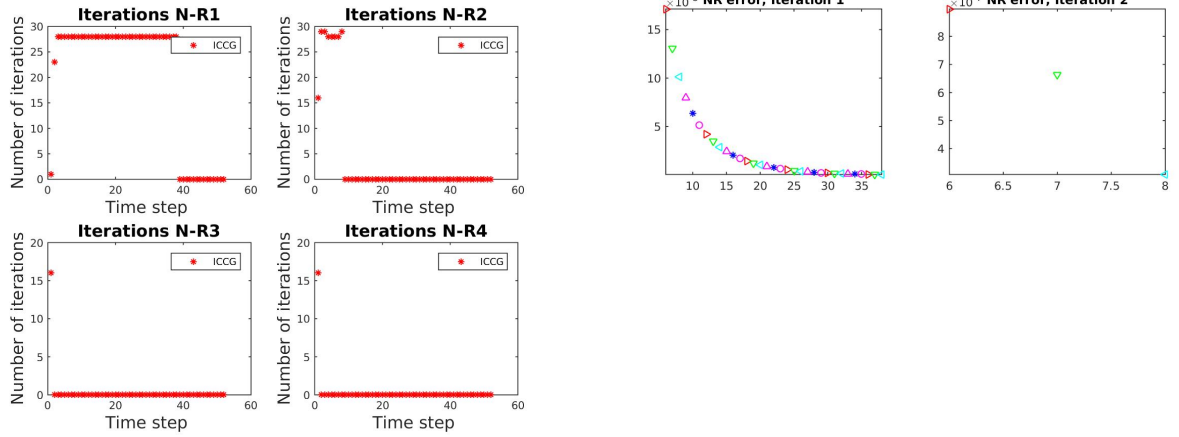


Figure 2: Number of iterations of the ICCG method for the first four NR iterations, accuracy NR iteration 10^{-4} .

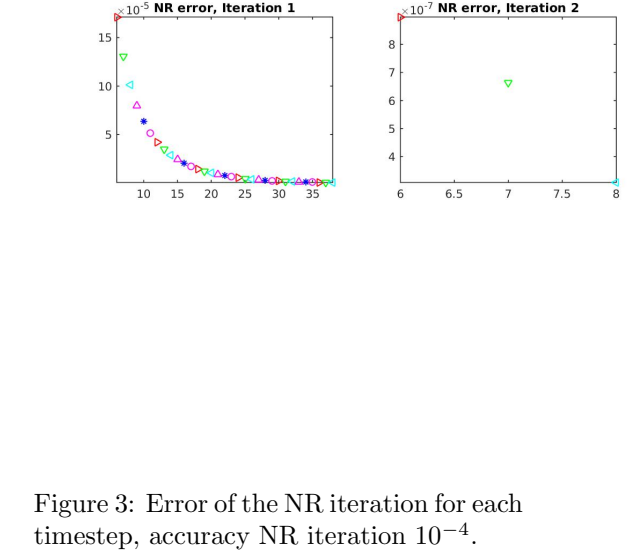


Figure 3: Error of the NR iteration for each timestep, accuracy NR iteration 10^{-4} .

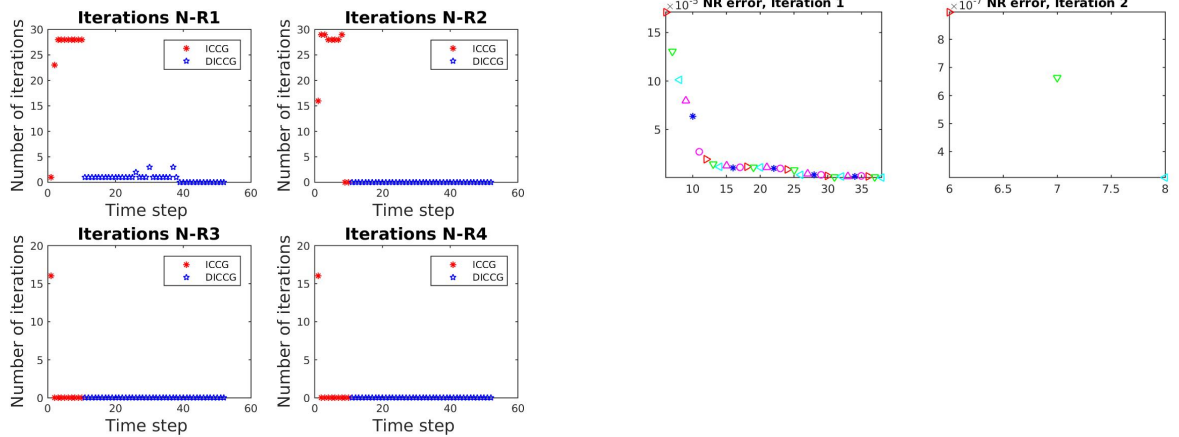


Figure 4: Number of iterations of the DICCG method for the first four NR iterations, accuracy NR iteration 10^{-4} .

Figure 5: Error of the NR iteration for each timestep, accuracy NR iteration 10^{-4} .

2 Accuracy NR iteration 10^{-5}

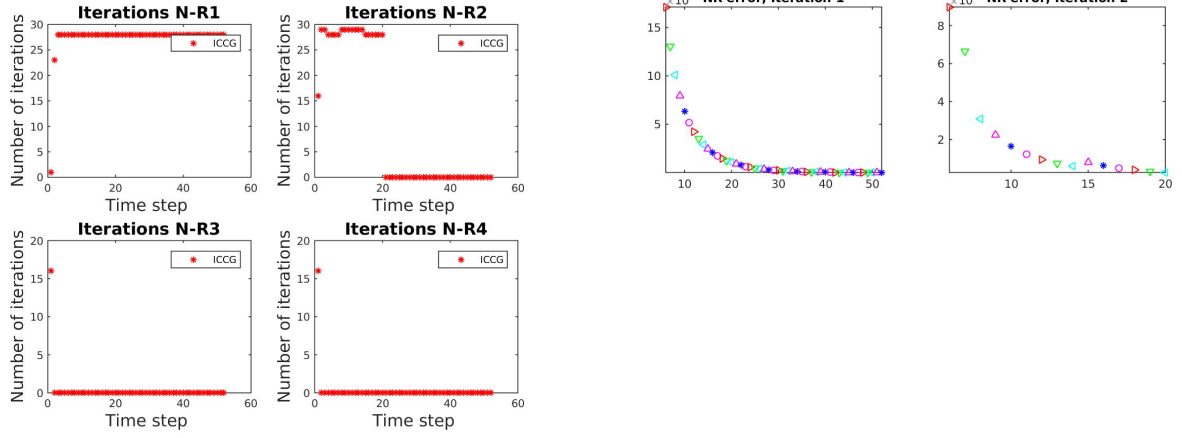


Figure 6: Number of iterations of the ICCG method for the first four NR iterations, accuracy NR iteration 10^{-5} .

Figure 7: Error of the NR iteration for each timestep, accuracy NR iteration 10^{-5} .

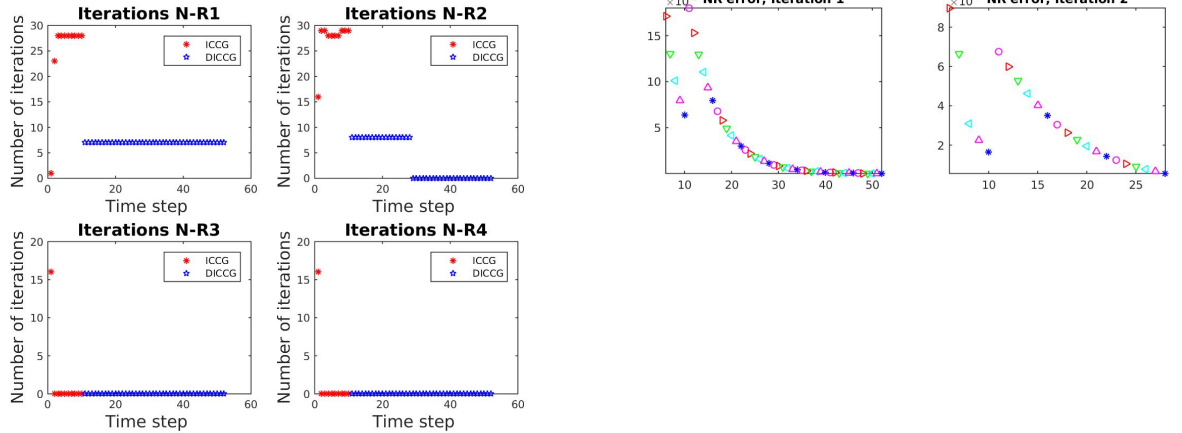


Figure 8: Number of iterations of the DICCG method for the first four NR iterations, accuracy NR iteration 10^{-4} .

Figure 9: Error of the NR iteration for each timestep, accuracy NR iteration 10^{-4} .

3 Accuracy NR iteration 10^{-6}

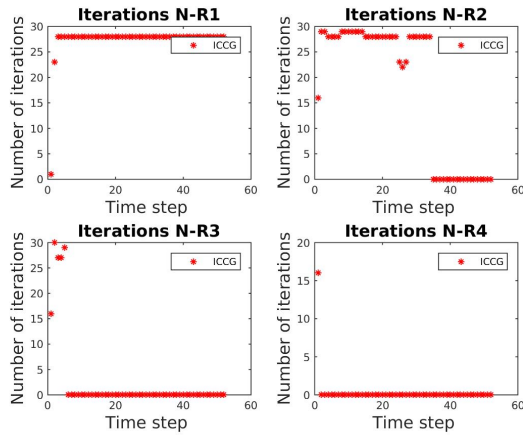


Figure 10: Number of iterations of the ICCG method for the first four NR iterations, accuracy NR iteration 10^{-6} .

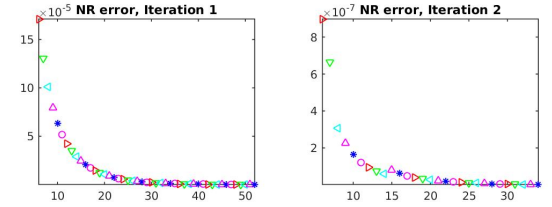


Figure 11: Error of the NR iteration for each timestep, accuracy NR iteration 10^{-6} .

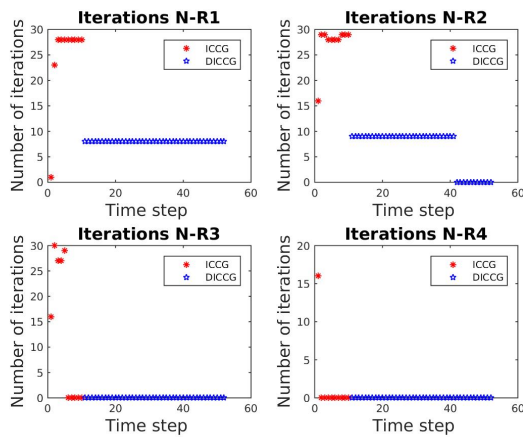


Figure 12: Number of iterations of the DICCG method for the first four NR iterations, accuracy NR iteration 10^{-6} .

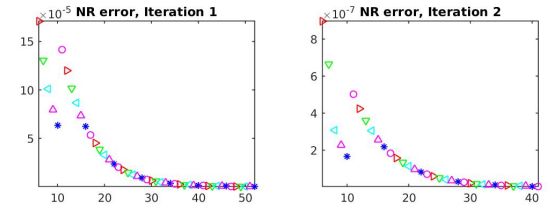


Figure 13: Error of the NR iteration for each timestep, accuracy NR iteration 10^{-6} .

4 Accuracy NR iteration 10^{-7}

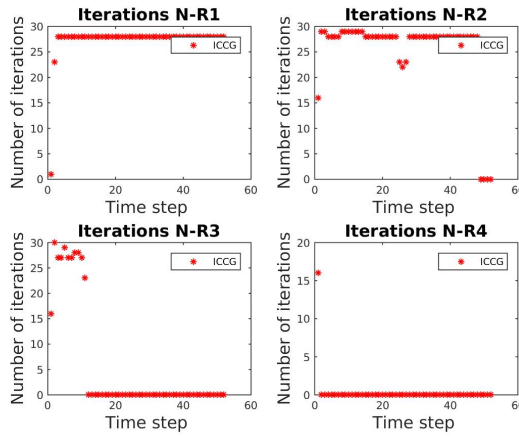


Figure 14: Number of iterations of the ICCG method for the first four NR iterations, accuracy NR iteration 10^{-7} .

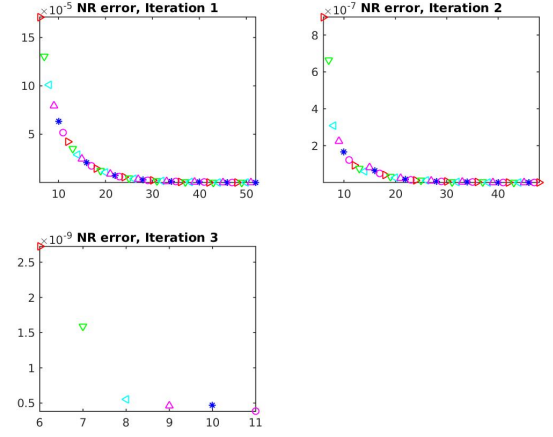


Figure 15: Error of the NR iteration for each timestep, accuracy NR iteration 10^{-7} .

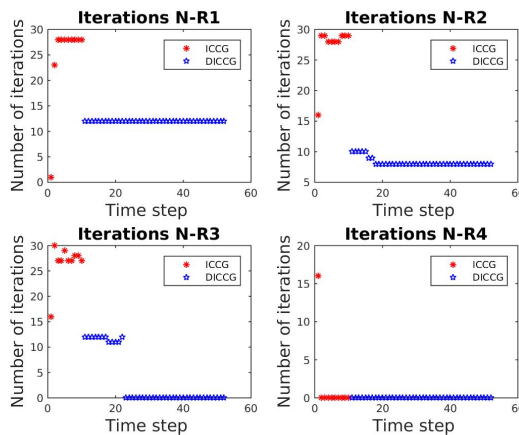


Figure 16: Number of iterations of the DICCG method for the first four NR iterations, accuracy NR iteration 10^{-7} .

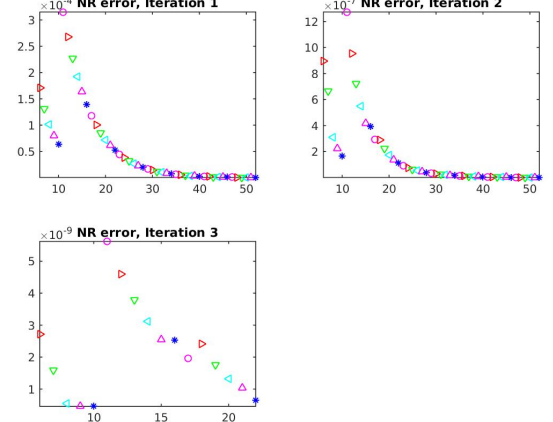


Figure 17: Error of the NR iteration for each timestep, accuracy NR iteration 10^{-7} .

5 Size 35 x 35

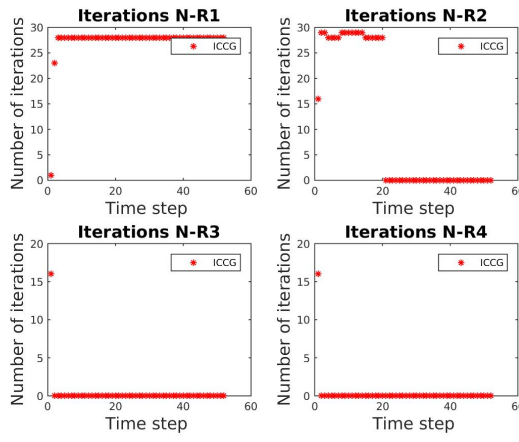


Figure 18: Number of iterations of the ICCG method for the first four NR iterations, size 35 x 35.

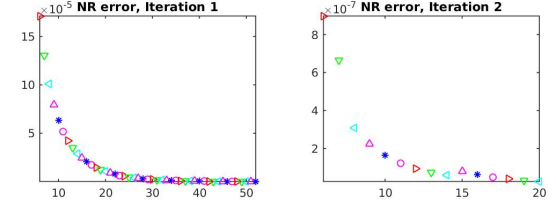


Figure 19: Error of the NR iteration for each timestep, size 35 x 35.

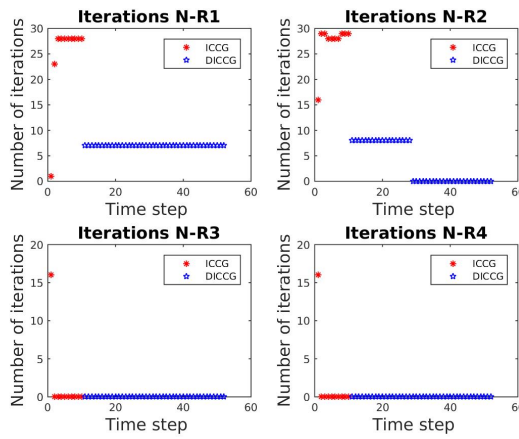


Figure 20: Number of iterations of the DICCG method for the first four NR iterations, size 35 x 35.

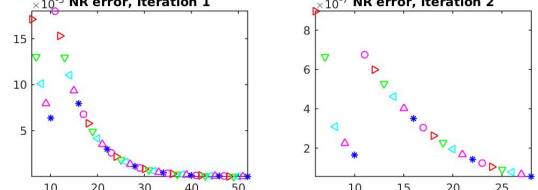


Figure 21: Error of the NR iteration for each timestep, size 35 x 35.

6 Size 70 x 70

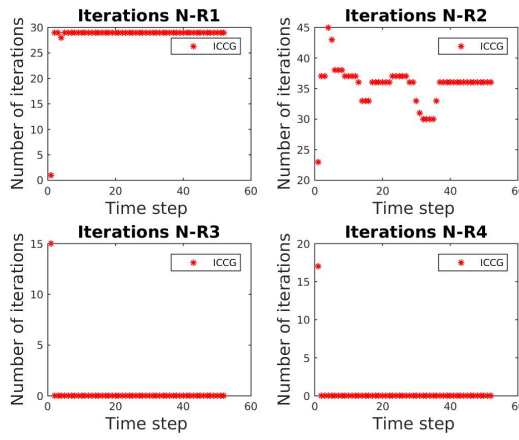


Figure 22: Number of iterations of the ICCG method for the first four NR iterations, size 70 x 70.

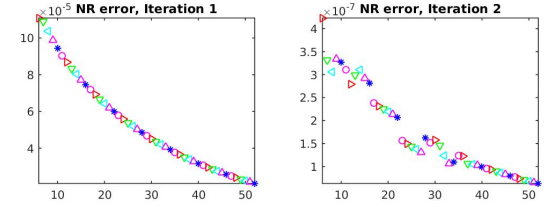


Figure 23: Error of the NR iteration for each timestep, size 70 x 70.

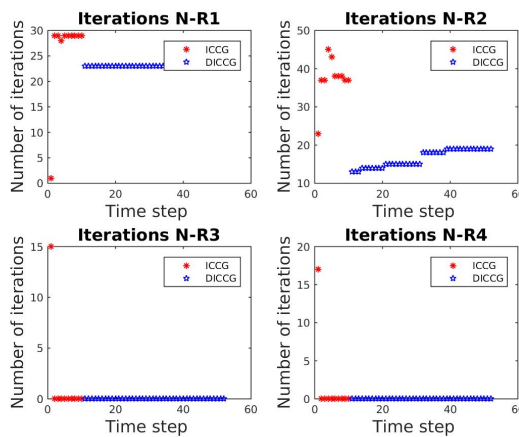


Figure 24: Number of iterations of the DICCG method for the first four NR iterations, size 70 x 70.

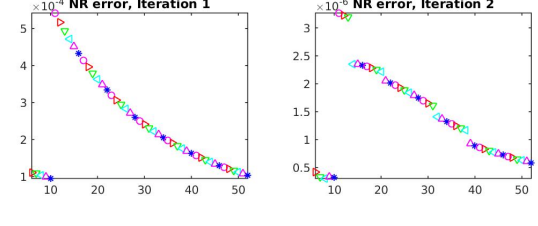


Figure 25: Error of the NR iteration for each timestep, size 70 x 70.

7 Size 70 x 70

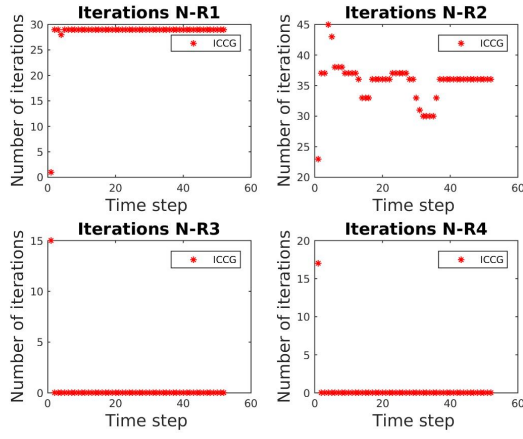


Figure 26: Number of iterations of the ICCG method for the first four NR iterations, size 70 x 70.

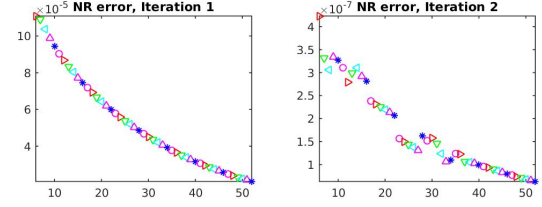


Figure 27: Error of the NR iteration for each timestep, size 70 x 70.

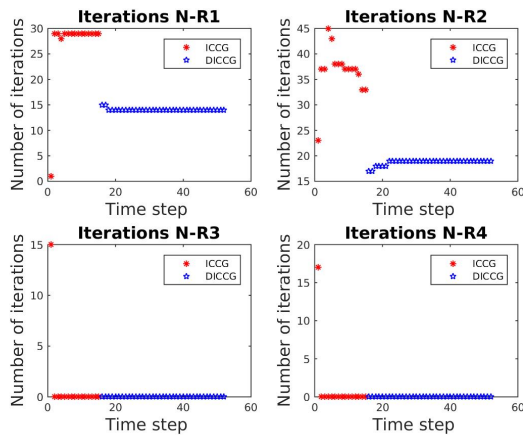


Figure 28: Number of iterations of the DICCG method for the first four NR iterations, size 70 x 70, 15 deflation vectors.

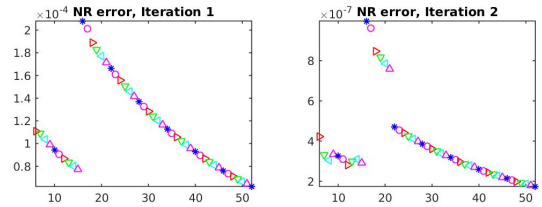


Figure 29: Error of the NR iteration for each timestep, size 70 x 70, 15 deflation vectors.

8 Size 105 x 105

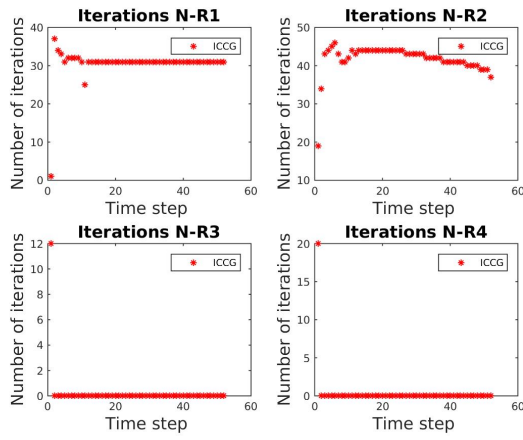


Figure 30: Number of iterations of the ICCG method for the first four NR iterations, size 105 x 105.

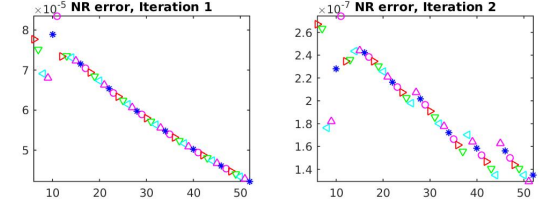


Figure 31: Error of the NR iteration for each timestep, size 105 x 105.

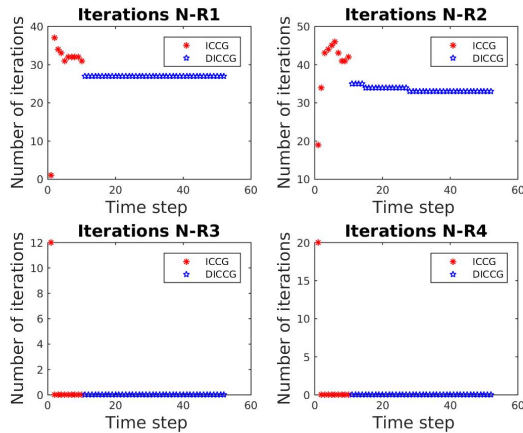


Figure 32: Number of iterations of the DICCG method for the first four NR iterations, size 105 x 105.

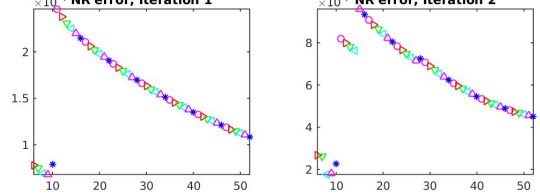


Figure 33: Error of the NR iteration for each timestep, size 105 x 105.

9 Size 105 x 105

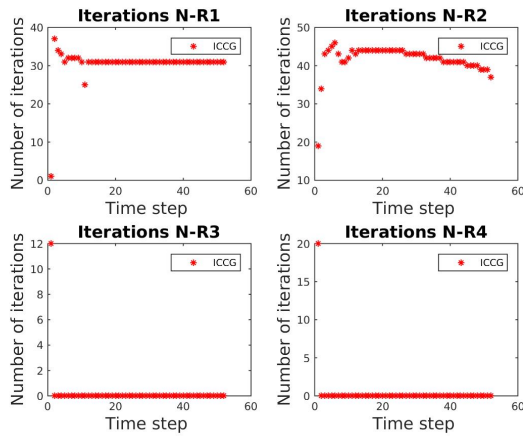


Figure 34: Number of iterations of the ICCG method for the first four NR iterations, size 105 x 105.

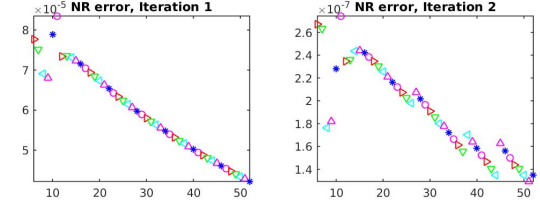


Figure 35: Error of the NR iteration for each timestep, size 105 x 105.

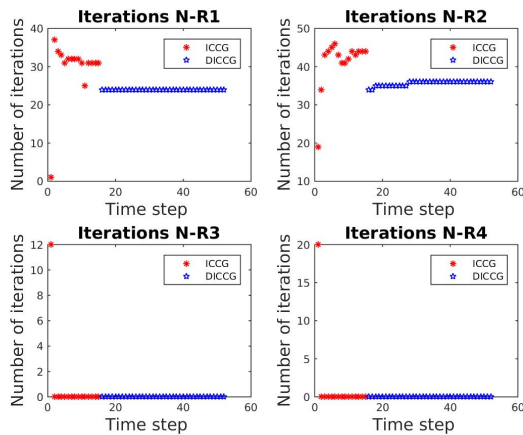


Figure 36: Number of iterations of the DICCG method for the first four NR iterations, size 105 x 105, 15 deflation vectors.

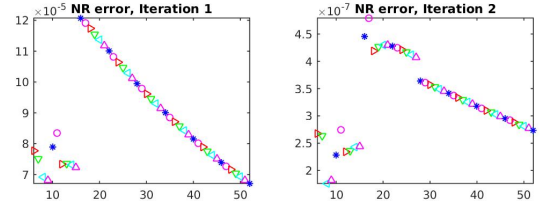


Figure 37: Error of the NR iteration for each timestep, size 105 x 105, 15 deflation vectors.

10 Size 105 x 105

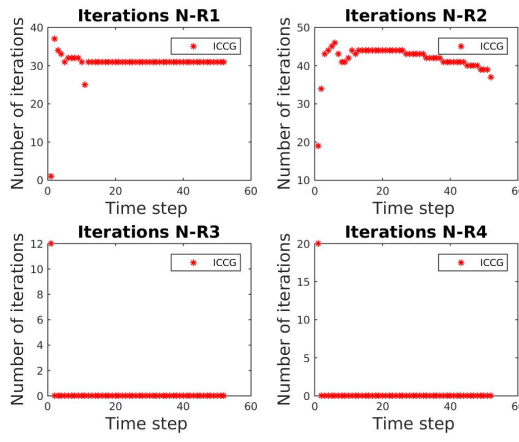


Figure 38: Number of iterations of the ICCG method for the first four NR iterations, size 105 x 105.

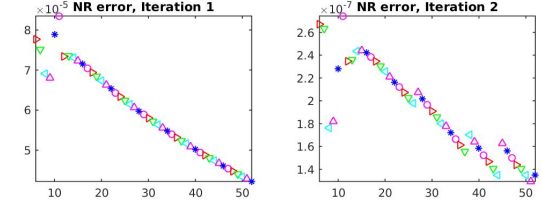


Figure 39: Error of the NR iteration for each timestep, size 105 x 105.

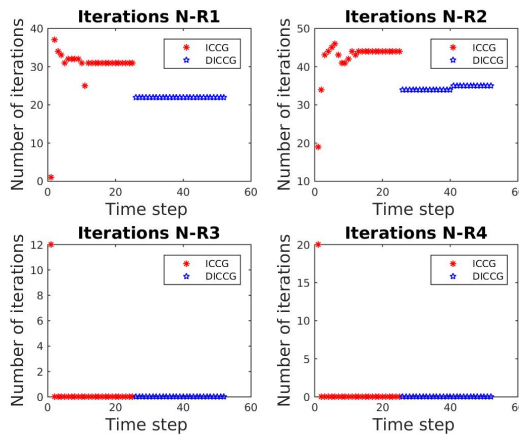


Figure 40: Number of iterations of the DICCG method for the first four NR iterations, size 105 x 105, 25 deflation vectors, POD (10-25).

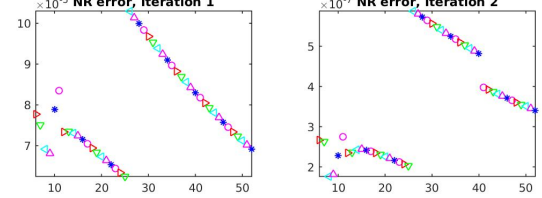


Figure 41: Error of the NR iteration for each timestep, size 105 x 105, 25 deflation vectors, POD (10-25).

11 Contrast in permeability 10^{-1}

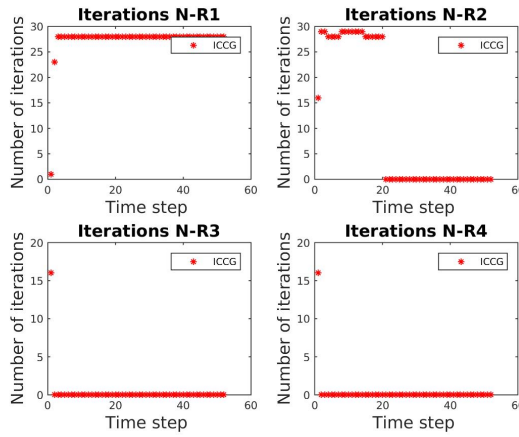


Figure 42: Number of iterations of the ICCG method for the first four NR iterations, size 35×35 , contrast in permeability 10^{-1} .

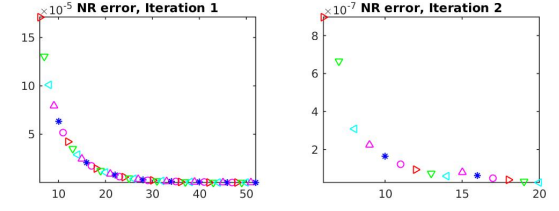


Figure 43: Error of the NR iteration for each timestep, size 35×35 , contrast in permeability 10^{-1} .

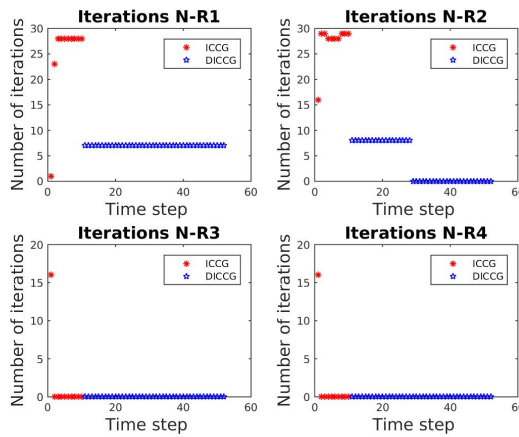


Figure 44: Number of iterations of the DICCG method for the first four NR iterations, size 35×35 , contrast in permeability 10^{-1} .

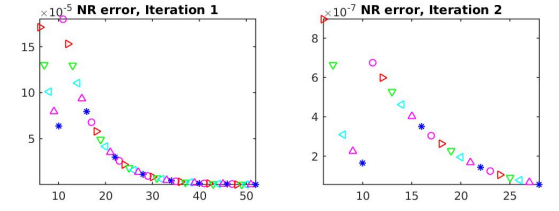


Figure 45: Error of the NR iteration for each timestep, size 35×35 , contrast in permeability 10^{-1} .

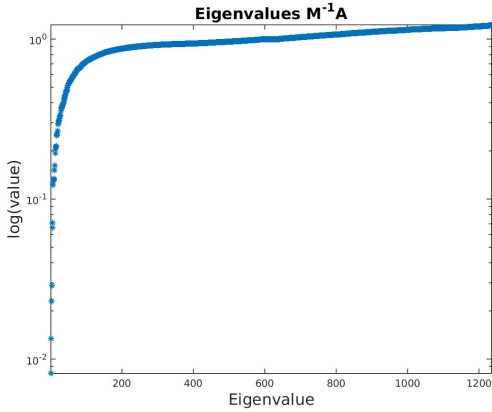


Figure 46: Eigenvalues of the preconditioned system ICCG.

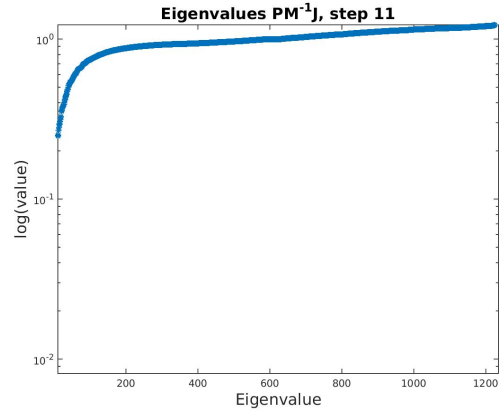


Figure 47: Eigenvalues of the deflated system DICCG₁₀ with 10 deflation vectors.

12 Contrast in permeability 10^{-2}

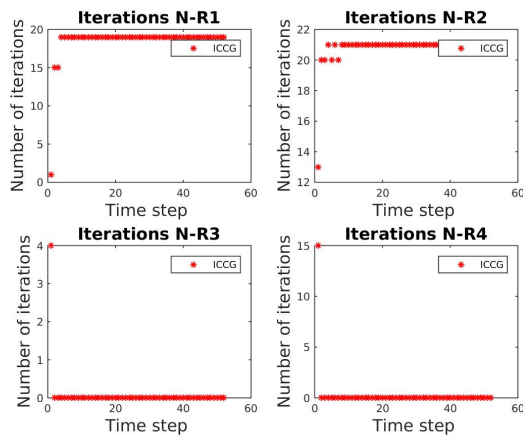


Figure 48: Number of iterations of the ICCG method for the first four NR iterations, size 35 x 35, contrast in permeability 10^{-2} .

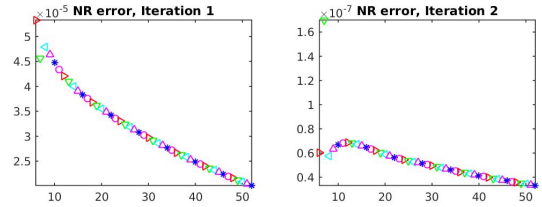


Figure 49: Error of the NR iteration for each timestep, size 35 x 35, contrast in permeability 10^{-2} .

12.1 10 deflation vectors

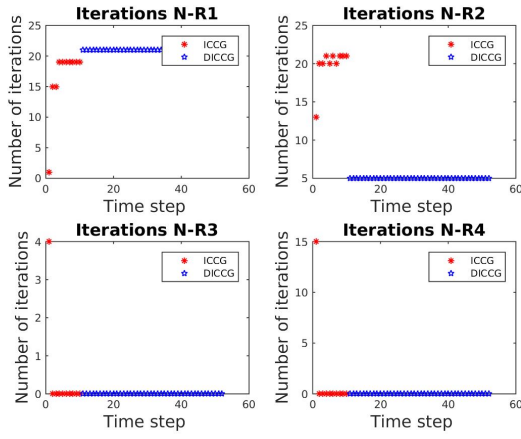


Figure 50: Number of iterations of the DICCG method for the first four NR iterations, size 35×35 , contrast in permeability 10^{-2} .

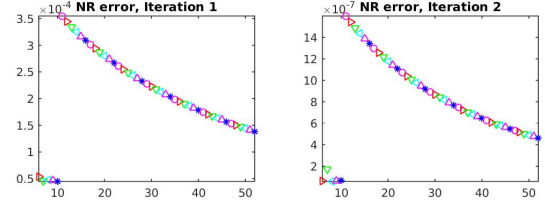


Figure 51: Error of the NR iteration for each timestep, size 35×35 , contrast in permeability 10^{-2} .

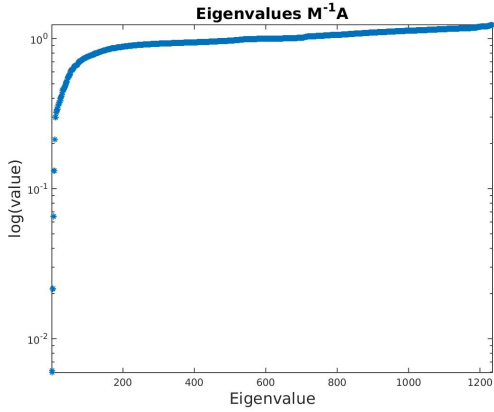


Figure 52: Eigenvalues of the preconditioned system ICCG.

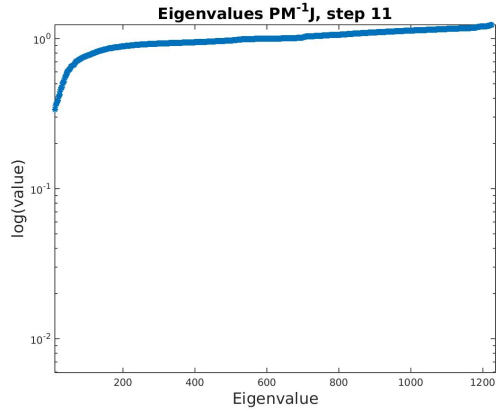


Figure 53: Eigenvalues of the deflated system DICCG₁₀ with 10 deflation vectors.

12.2 20 deflation vectors, 15 POD vectors

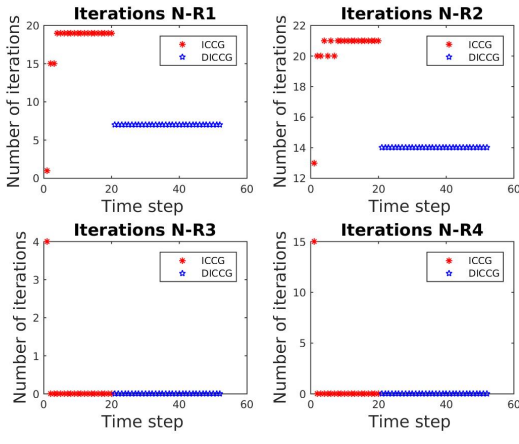


Figure 54: Number of iterations of the $\text{DICCG}_{\text{POD}15}$ method for the first four NR iterations, size 35×35 , contrast in permeability 10^{-2} .

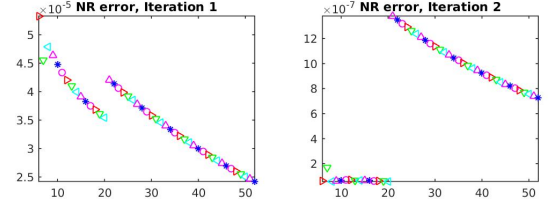


Figure 55: Error of the NR iteration for each timestep, size 35×35 , contrast in permeability 10^{-2} .

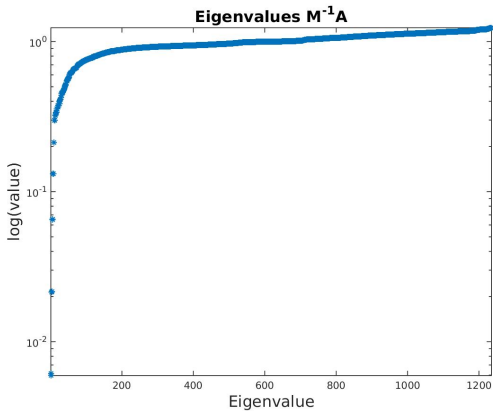


Figure 56: Eigenvalues of the preconditioned system ICCG.

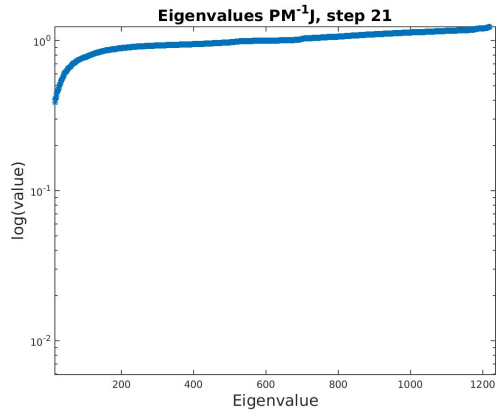


Figure 57: Eigenvalues of the deflated system $\text{DICCG}_{\text{POD}15}$ with 15 POD basis vectors obtained from 20 deflation vectors.

13 Contrast in permeability 10^{-3}

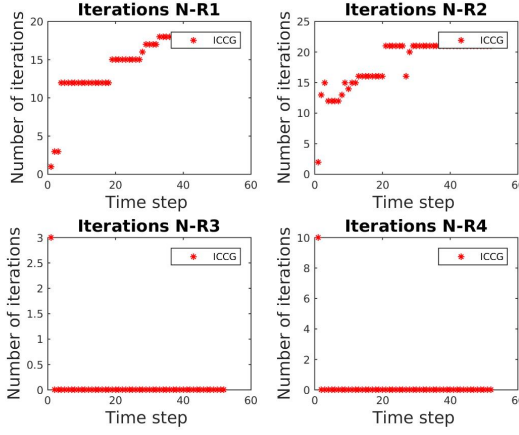


Figure 58: Number of iterations of the ICCG method for the first four NR iterations, size 35×35 , contrast in permeability 10^{-3} .

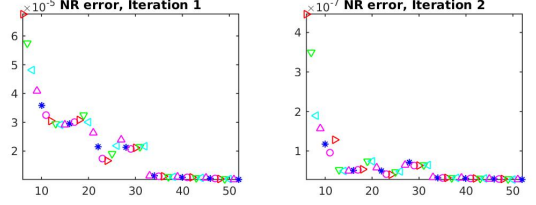


Figure 59: Error of the NR iteration for each timestep, size 35×35 , contrast in permeability 10^{-3} .

13.1 20 deflation vectors, 15 POD vectors

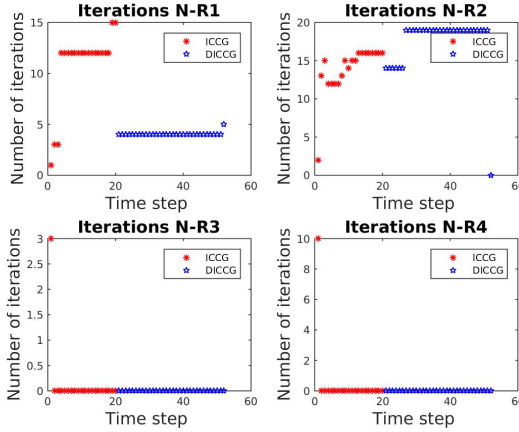


Figure 60: Number of iterations of the DICCG_{POD15} method for the first four NR iterations, size 35×35 , contrast in permeability 10^{-3} .

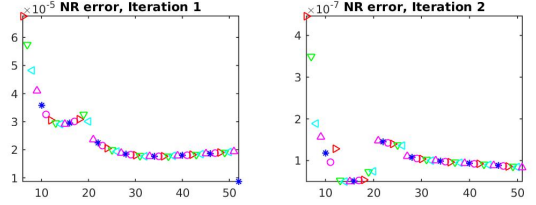


Figure 61: Error of the NR iteration for each timestep, size 35×35 , contrast in permeability 10^{-3} .

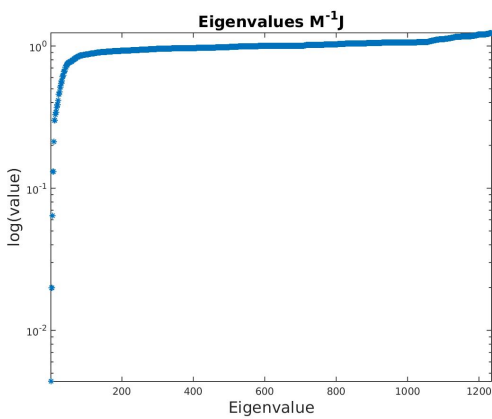


Figure 62: Eigenvalues of the preconditioned system ICCG.

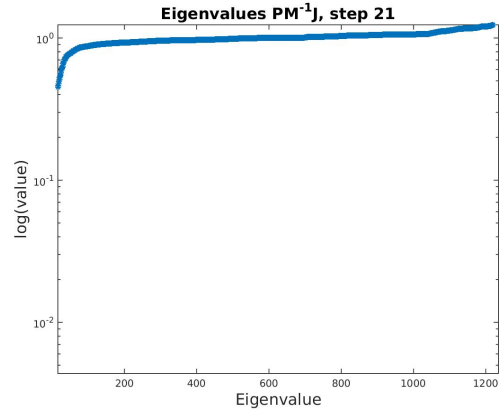


Figure 63: Eigenvalues of the deflated system DICCG_{POD15} with 15 POD basis vectors obtained from 20 deflation vectors.

13.2 30 deflation vectors, 25 POD vectors

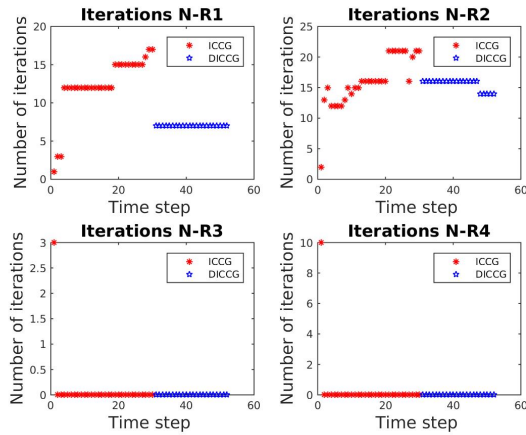


Figure 64: Number of iterations of the DICCG_{POD15} method for the first four NR iterations, size 35 x 35, contrast in permeability 10^{-3} .

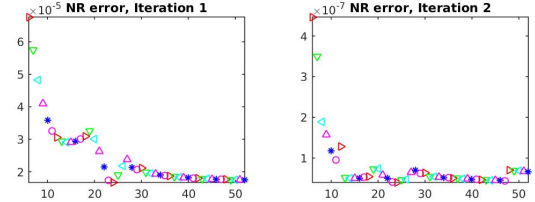


Figure 65: Error of the NR iteration for each timestep, size 35 x 35, contrast in permeability 10^{-3} .

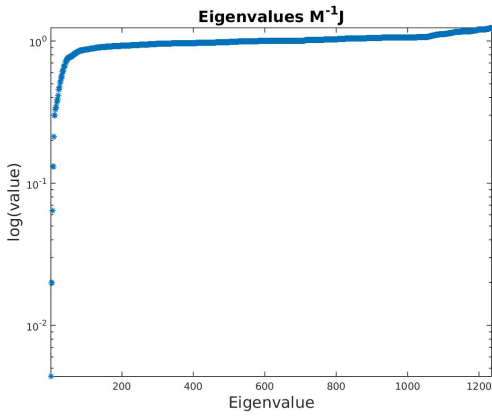


Figure 66: Eigenvalues of the preconditioned system ICCG.

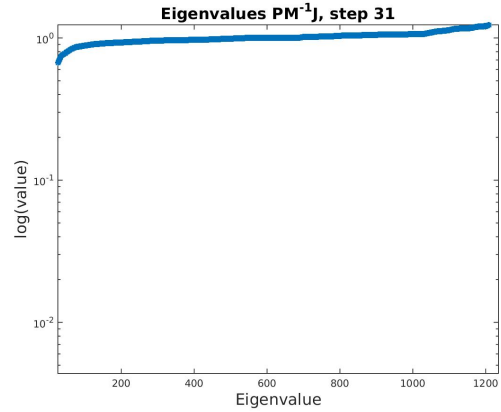


Figure 67: Eigenvalues of the deflated system $DICCG_{POD15}$ with 15 POD basis vectors obtained from 20 deflation vectors.

14 NumSteps 13

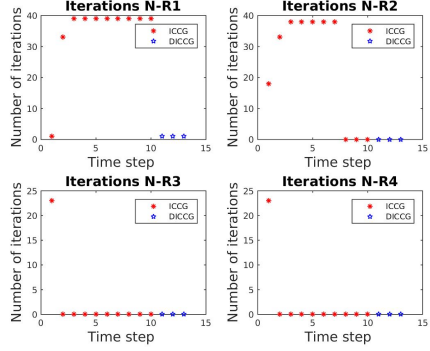


Figure 68: Number of iterations of the $DICCG_{10}$ method for the first four NR iterations.

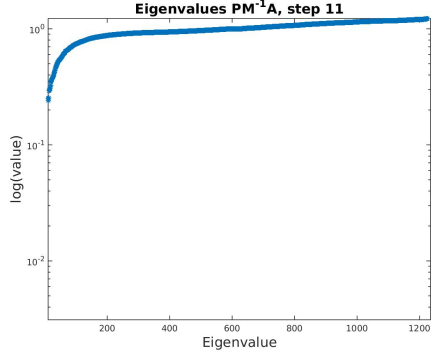


Figure 69: Eigenvalues of the deflated system $DICCG_{10}$ with 10 deflation vectors.

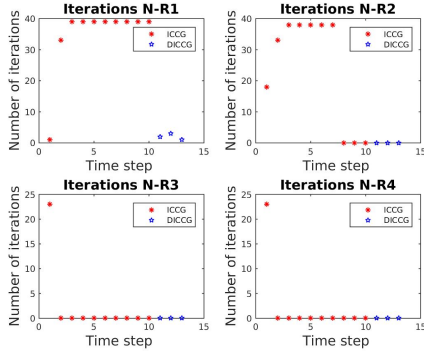


Figure 70: Number of iterations of the $DICCG_{POD}$ method for the first four NR iterations, eigenvectors [6-10].

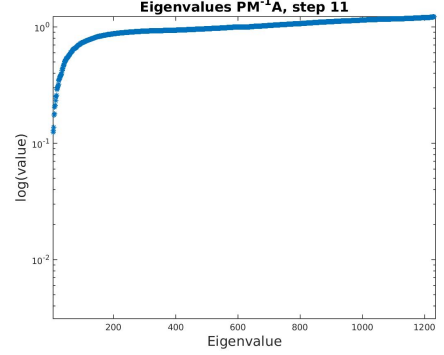


Figure 71: Eigenvalues of the deflated system $DICCG_{POD}$ with 10 deflation vectors, eigenvectors [6-10].

15 NumSteps 26

The eigenvalues of the matrices are presented in Figure 79 for the original system matrix \mathbf{J} for the first timestep, Figure 104 for the preconditioned system, Figure 106 the deflated system $DICCG_{10}$ and Figure 108 the deflated system combined with POD $DICCG_{POD}$ using the eigenvectors corresponding to the five largest eigenvalues. The eigenvalues of the snapshot correlation matrix $\mathbf{R} = \frac{1}{m}\mathbf{Z}\mathbf{Z}^T$ are presented in Figure 80.

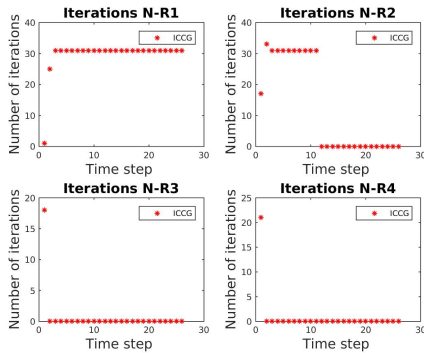


Figure 72: Number of iterations of the ICCG method for the first four NR iterations.

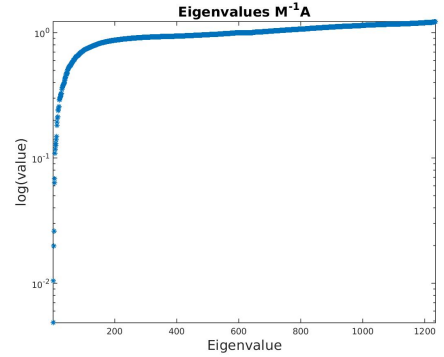


Figure 73: Eigenvalues of the preconditioned matrix, time step 1.

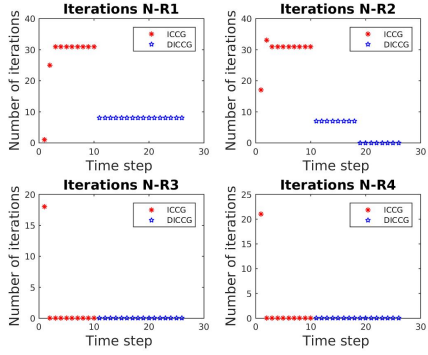


Figure 74: Number of iterations of the DICCG_{10} method for the first four NR iterations.

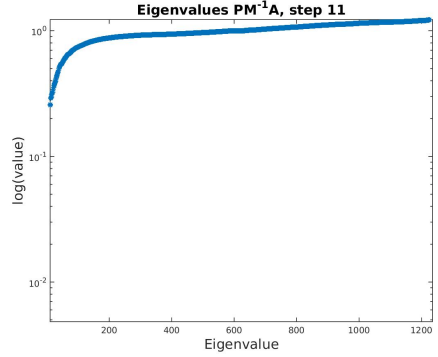


Figure 75: Eigenvalues of the deflated system DICCG_{10} with 10 deflation vectors.

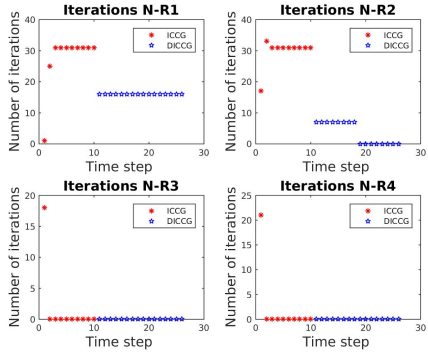


Figure 76: Number of iterations of the DICCG_{POD} method for the first four NR iterations, eigenvectors [6-10].

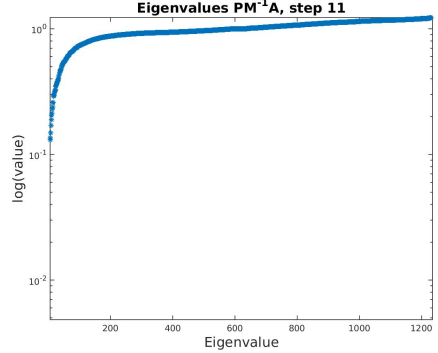


Figure 77: Eigenvalues of the deflated system DICCG_{POD} with 10 deflation vectors, eigenvectors [6-10].

16 NumSteps 52

The number of iterations necessary to reach convergence with the linear solvers is presented for the first four NR iterations in Figure 103 for the ICCG method, Figure 105 for the deflated method DICCG_{10} using 10 snapshots as deflation vectors and Figure 107, DICCG_{POD} , using the first 5 basis vectors of POD as deflation vectors. The eigenvalues of the matrices are presented in Figure 79 for the original system matrix \mathbf{J} for the first timestep, Figure 104 for the preconditioned system, Figure 106 the deflated system DICCG_{10} and Figure 108 the deflated system combined with POD DICCG_{POD} using the eigenvectors corresponding to the five largest eigenvalues. The eigenvalues of the

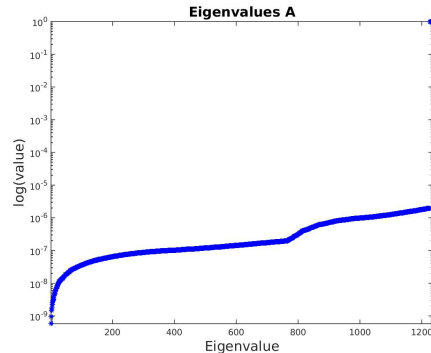


Figure 79: Eigenvalues of the original matrix \mathbf{J} , time step 1.

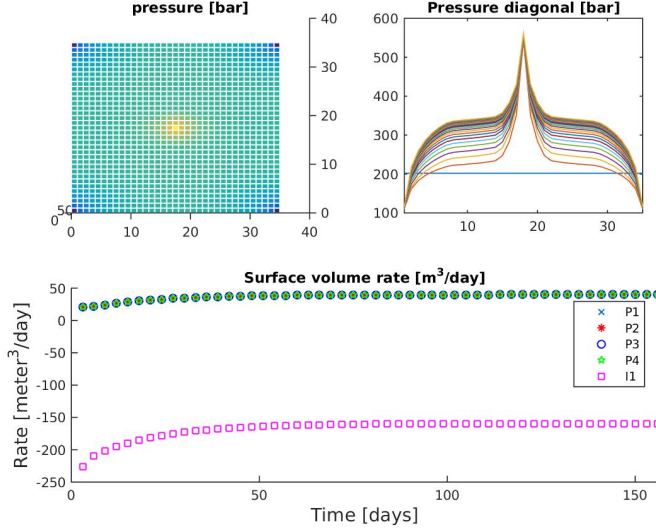


Figure 78: Solution of the compressible problem solved with the ICCG method.

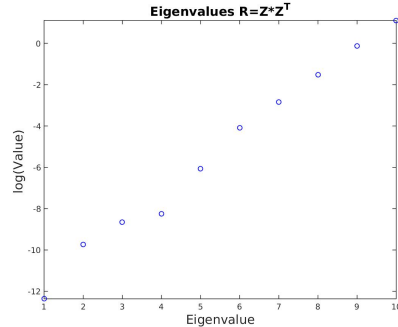


Figure 80: Eigenvalues of POD matrix, 10 deflation vectors.

snapshot correlation matrix $\mathbf{R} = \frac{1}{m} \mathbf{Z} \mathbf{Z}^T$ are presented in Figure 80.

We observe that the number of iterations for the first and second NR iterations is lower for the deflated methods compared with the ICCG method. However, we observe that the time step when convergence is achieved for the NR cycle is larger for these methods with respect to the ICCG method. We also observe that for the first NR iteration, the decrease is larger for the deflated method with 10 snapshots as deflation vectors.

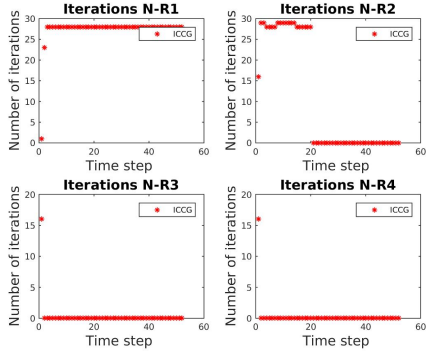


Figure 81: Number of iterations of the ICCG method for the first four NR iterations.

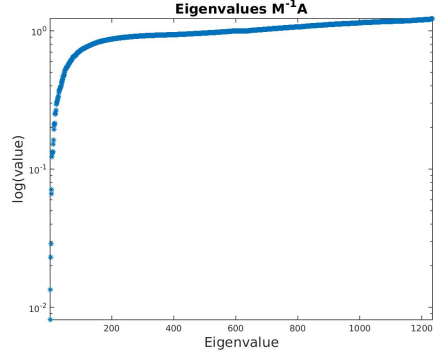


Figure 82: Eigenvalues of the preconditioned matrix, time step 1.

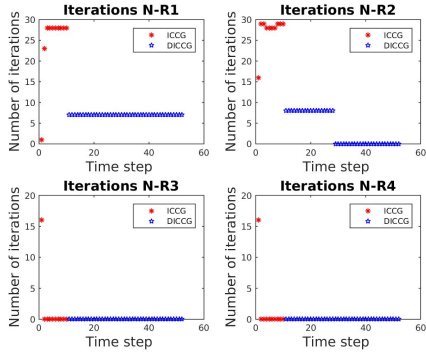


Figure 83: Number of iterations of the DICCG₁₀ method for the first four NR iterations.

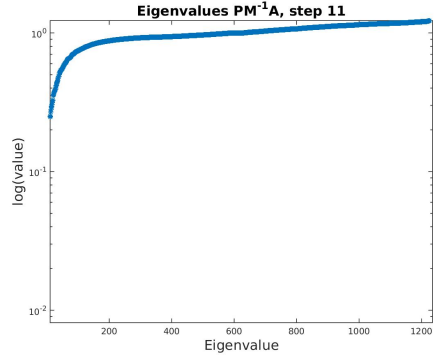


Figure 84: Eigenvalues of the deflated system DICCG₁₀ with 10 deflation vectors.

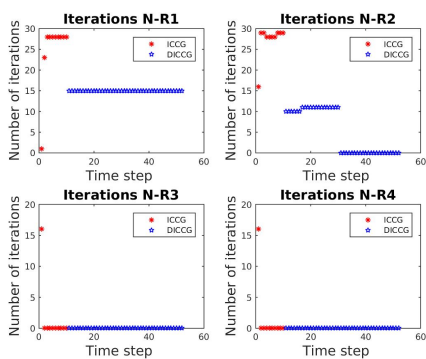


Figure 85: Number of iterations of the DICCG_{POD} method for the first four NR iterations, eigenvectors [6-10].

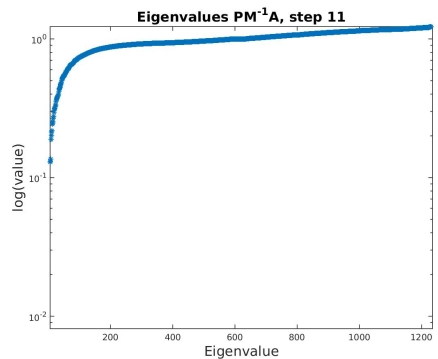


Figure 86: Eigenvalues of the deflated system DICCG_{POD} with 10 deflation vectors, eigenvectors [6-10].

17 NumSteps 104

17.1 10 Def vectors

The eigenvalues of the matrices are presented in Figure 79 for the original system matrix \mathbf{J} for the first timestep, Figure 104 for the preconditioned system, Figure 106 the deflated

system $DICCG_{10}$ and Figure 108 the deflated system combined with POD $DICCG_{POD}$ using the eigenvectors corresponding to the five largest eigenvalues. The eigenvalues of the snapshot correlation matrix $\mathbf{R} = \frac{1}{m}\mathbf{Z}\mathbf{Z}^T$ are presented in Figure 80.

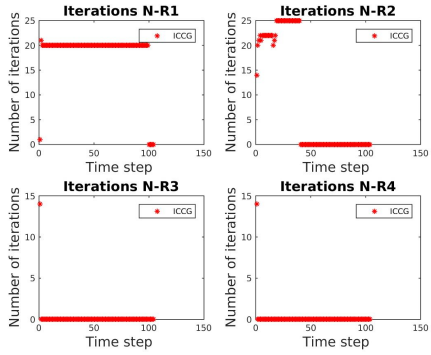


Figure 87: Number of iterations of the ICCG method for the first four NR iterations.

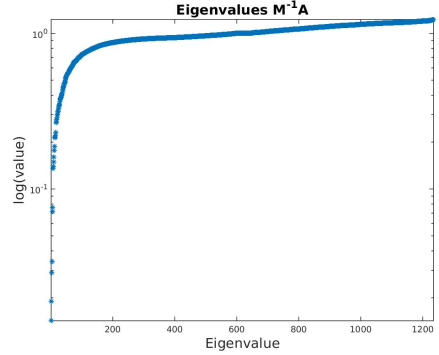


Figure 88: Eigenvalues of the preconditioned matrix, time step 1.

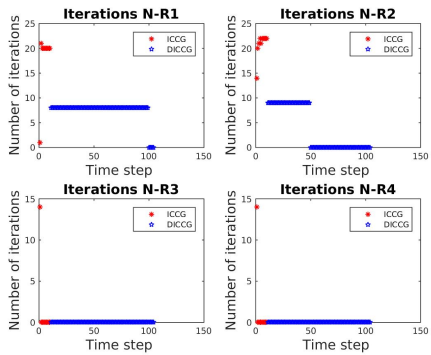


Figure 89: Number of iterations of the $DICCG_{10}$ method for the first four NR iterations.

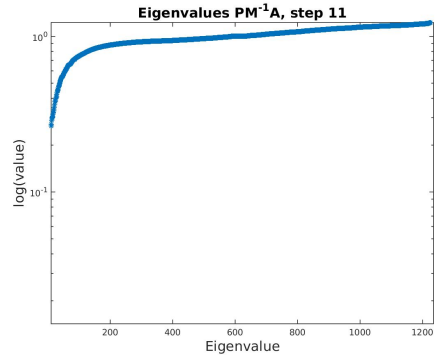


Figure 90: Eigenvalues of the deflated system $DICCG_{10}$ with 10 deflation vectors.

17.2 20 deflation vectors

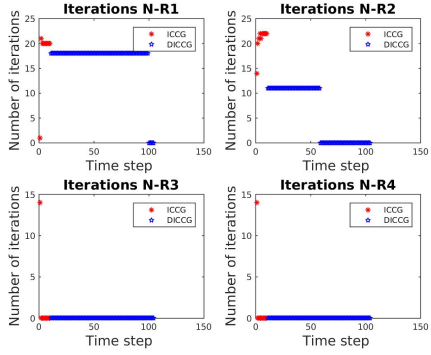


Figure 91: Number of iterations of the $DICCG_{POD}$ method for the first four NR iterations, eigenvectors [6-10].

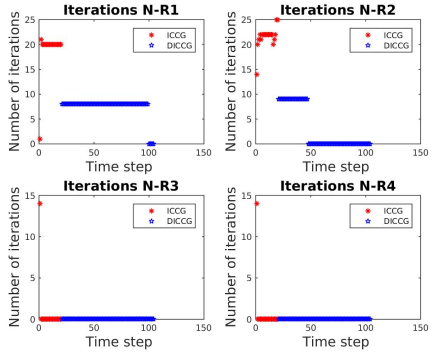


Figure 93: Number of iterations of the $DICCG_{20}$ method for the first four NR iterations.

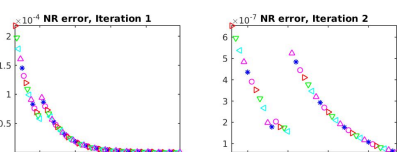


Figure 95: Error of the NR iteration.

18 NumSteps 156

The eigenvalues of the matrices are presented in Figure 79 for the original system matrix \mathbf{J} for the first timestep, Figure 104 for the preconditioned system, Figure 106 the deflated

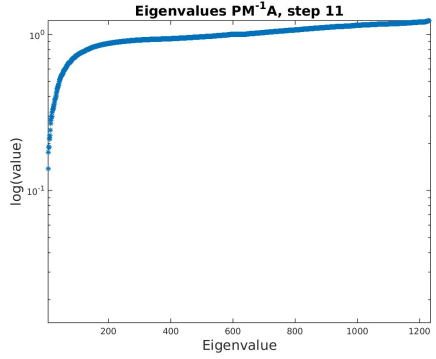


Figure 92: Eigenvalues of the deflated system $DICCG_{POD}$ with 10 deflation vectors, eigenvectors [6-10].

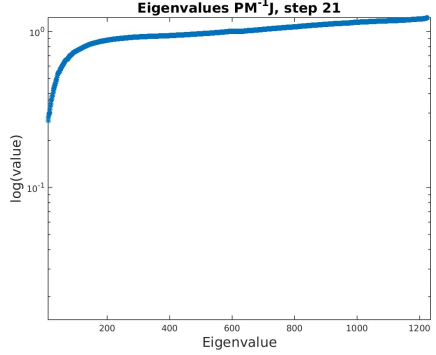


Figure 94: Eigenvalues of the deflated system $DICCG_{20}$ with 10 POD deflation vectors.

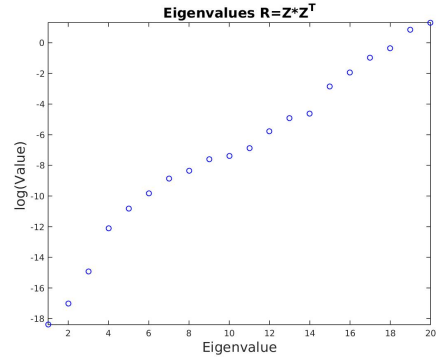


Figure 96: Eigenvalues of the correlation matrix $X = Z * Z'$.

system $DICCG_{10}$ and Figure 108 the deflated system combined with POD $DICCG_{POD}$ using the eigenvectors corresponding to the five largest eigenvalues. The eigenvalues of the snapshot correlation matrix $\mathbf{R} = \frac{1}{m}\mathbf{Z}\mathbf{Z}^T$ are presented in Figure 80.

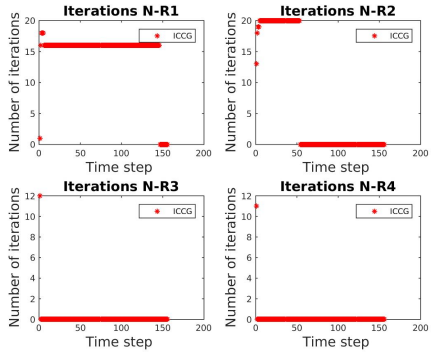


Figure 97: Number of iterations of the ICCG method for the first four NR iterations.

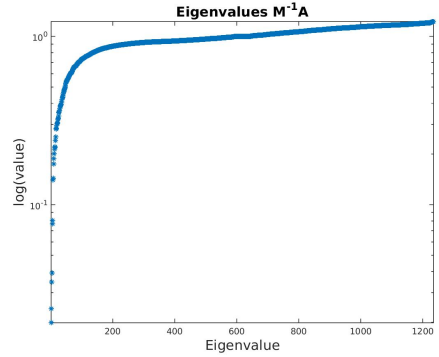


Figure 98: Eigenvalues of the preconditioned matrix, time step 1.

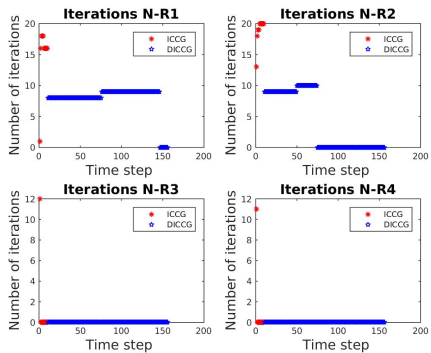


Figure 99: Number of iterations of the $DICCG_{10}$ method for the first four NR iterations.

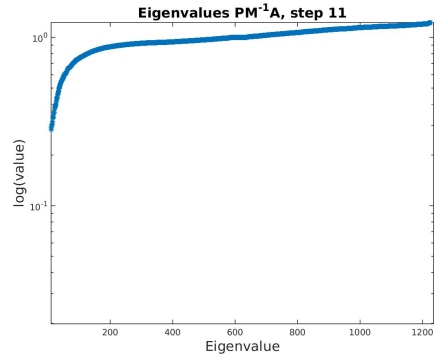


Figure 100: Eigenvalues of the deflated system $DICCG_{10}$ with 10 deflation vectors.

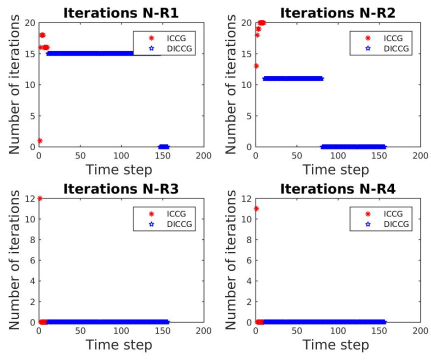


Figure 101: Number of iterations of the $\text{DICCG}_{\text{POD}}$ method for the first four NR iterations, eigenvectors [6-10].

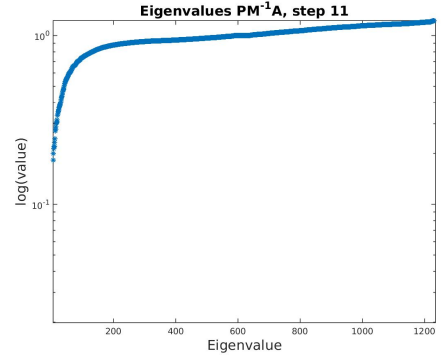


Figure 102: Eigenvalues of the deflated system $\text{DICCG}_{\text{POD}}$ with 10 deflation vectors, eigenvectors [6-10].

19 Update deflation vectors

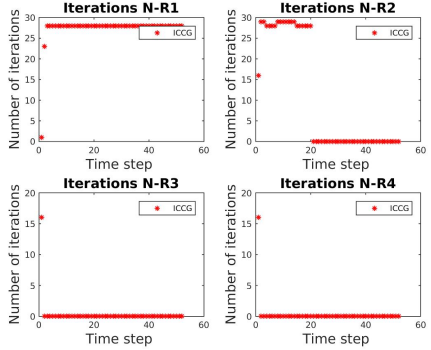


Figure 103: Number of iterations of the ICCG method for the first four NR iterations.

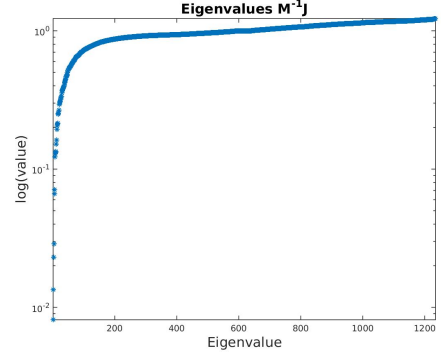


Figure 104: Eigenvalues of the preconditioned matrix, time step 1.

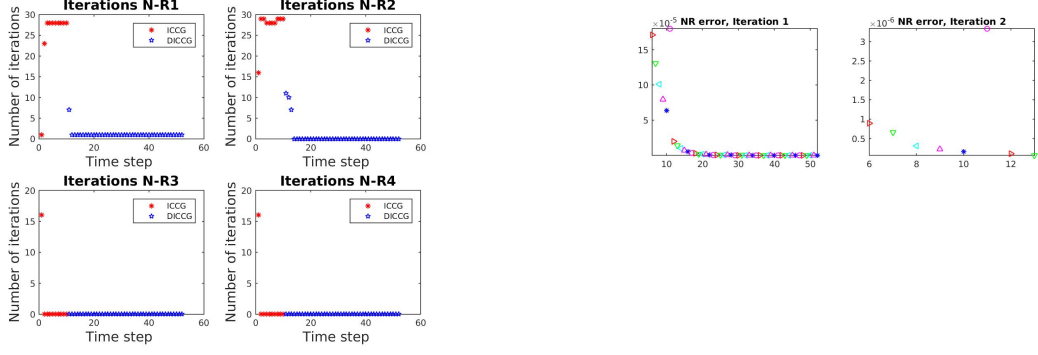


Figure 105: Number of iterations of the DICCG_{10} method for the first four NR iterations.

Figure 106: Eigenvalues of the deflated system DICCG_{10} with 10 deflation vectors.

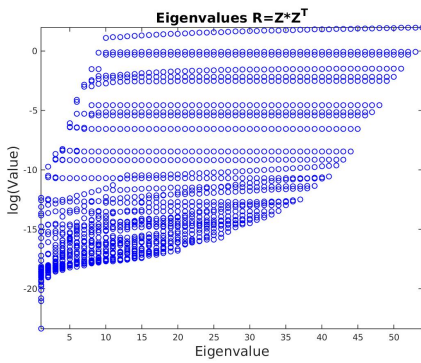


Figure 107: Eigenvalues of the matrix $X = Z * Z'$.

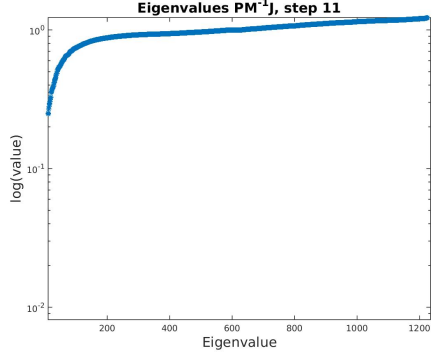


Figure 108: Eigenvalues of the deflated system DICCG_{POD} with 10 POD deflation vectors updated each timestep.

Case 2

In the second case, we compute the first 4 time steps varying the bhp of the wells, as described above. Figure 109 presents the solution obtained with ICCG method is presented. The upper left figure represents the pressure field at the final time step. The upper right figure represents the pressure across the diagonal joining the $(0,0)$ and $(35,35)$ grid cells. We can observe the initial pressure (200 bars) in this diagonal and the evolution of the pressure field through the time. In the lower figure, we observe the surface volume rate for the five wells during the simulation.

The number of iterations necessary to achieve convergence with the linear solvers for this second problem is presented for the first four NR iterations in Figure 110 for the ICCG method, Figure 111 for the deflated method DICCG_{10} using 10 snapshots as deflation vectors and Figure 112 DICCG_{POD} using 5 basis vectors of POD as deflation vectors.

As in the previous case, we observe that the number of iterations for the first and second NR iterations is lower for the deflated methods compared with the ICCG method. However, we observe that the time step when convergence is achieved for the NR cycle is

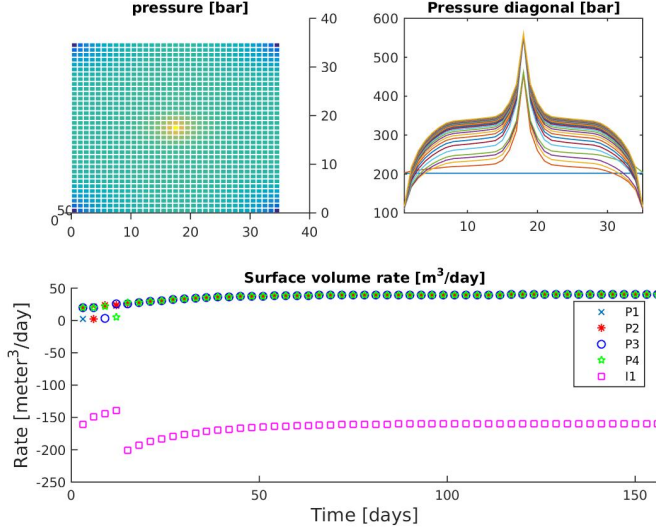


Figure 109: Solution of the compressible problem solved with the ICCG method, varying the bhp of the first 4 time steps.

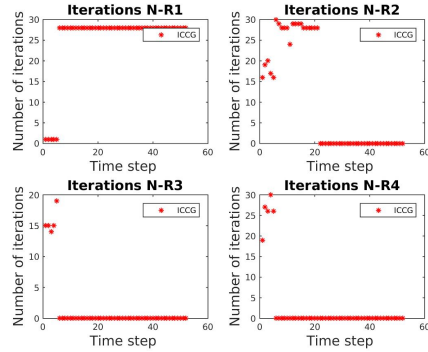


Figure 110: Number of iterations of the ICCG method for the first four NR iterations.

larger for these methods with respect to the ICCG method. We also observe that for the first NR iteration, the reduction is larger for the deflated method with 10 snapshots as deflation vectors.

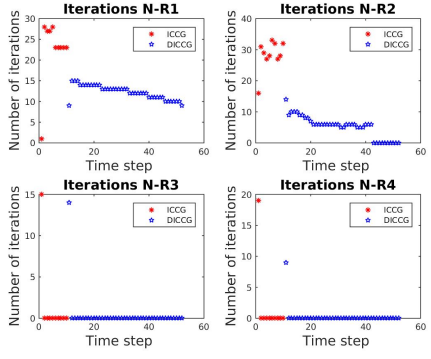


Figure 111: Number of iterations of the DICCG_{10} method for the first four NR iterations.

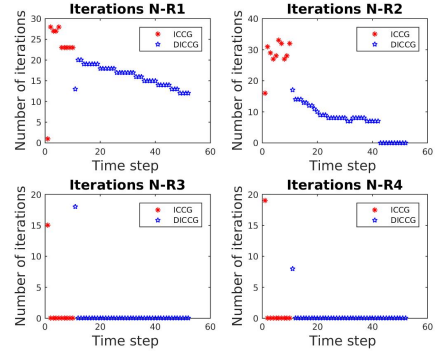


Figure 112: Number of iterations of the DICCG_{POD} method for the first four NR iterations.

References